Seismic and geodetic insights into magma accumulation at Katla subglacial volcano, Iceland: 1999 to 2005

Erik Sturkell,[1] Páll Einarsson,[2] Matthew J. Roberts,[3] Halldór Geirsson,[3] Magnús T. Gudmundsson,[2] Freysteinn Sigmundsson,[1] Virginie Pinel,[4] Gunnar B. Guðmundsson,[3] Halldór Ólafsson,[1] and Ragnar Stefánsson[5]

Received 10 November 2006; revised 12 September 2007; accepted 17 December 2007; published 27 March 2008.

[1] Katla is one of Iceland's most active volcanoes with at least 20 eruptions in the last 1100 years. The volcano is covered mostly by the Mýrdalsjökull ice cap; consequently, Katla eruptions are phreato-magmatic and are capable of producing jökulhlaups. A jökulhlaup in July 1999, preceded by an episode of continuous seismic tremor, was the first sign of renewed magma movement under the volcano since 1955. Using seismic and geodetic observations, and insights into geothermal activity from ice-surface observations, we analyze this period of unrest and assess the present state of Katla volcano. From 1999 to 2004, GPS measurements on nunataks exposed on the caldera edge revealed steady inflation of the volcano. Our measurements show uplift and horizontal displacement of the nuntatak benchmarks at a rate of up to 2 cm a^{-1}, together with horizontal displacement of far-field stations (>11 km) at about 0.5 cm a^{-1} away from the caldera centre. Using a point-source model, these data place the center of the magma chamber at 4.9 km depth beneath the northern part of the caldera. However, this depth may be overestimated because of a progressive decrease in the mass of the overlying ice cap. The depth may be only 2–3 km. About 0.01 km^3 of magma has accumulated between 1999 and 2004; this value is considerably less than the estimated 1 km^3 of material erupted during the last eruption of Katla in 1918. Presently, rates of crustal deformation and earthquake activity are considerably less than observed between 1999 and 2004; nonetheless, the volcano remains in an agitated state.

Citation: Sturkell, E., P. Einarsson, M. J. Roberts, H. Geirsson, M. T. Gudmundsson, F. Sigmundsson, V. Pinel, G. B. Guðmundsson, H. Ólafsson, and R. Stefánsson (2008), Seismic and geodetic insights into magma accumulation at Katla subglacial volcano, Iceland: 1999 to 2005, *J. Geophys. Res.*, *113*, B03212, doi:10.1029/2006JB004851.

1. Introduction

[2] Active, ice-covered volcanoes are located in the diverse geographical regions in Eurasia, the Americas, and Antarctica. Eruptions of such volcanoes can cause severe, far-reaching hazards such as glacier floods (jökulhlaup) and lahars due to sudden melting of ice [*Major and Newhall*, 1989]. In Iceland, subglacial volcanism is common, with the volcanoes Grímsvötn and Katla renowned for frequent eruptive activity (Figure 1). Katla volcano is located beneath the Mýrdalsjökull ice cap (Figure 2) and since settlement time, around 874 AD, it has erupted at least 20 times [*Larsen*, 2000]. Jökulhlaups and fallout of tephra are primary hazards during a Katla eruption, and the proximity of the volcano to populated areas and to international flight paths makes it a potent threat. In July 1999, an unexpected jökulhlaup drained from Mýrdalsjökull. This short-lived jökulhlaup was preceded several hours earlier by earthquakes and pulses of low-frequency tremor that originated from Mýrdalsjökull. Inspection of Mýrdalsjökull revealed a newly formed surface depression (ice cauldron) near to the epicenters of the earthquake swarm that preceded the jökulhlaup. The last Katla eruption to break the ice-surface occurred in 1918. This event was accompanied by a massive jökulhlaup, which emerged from the eastern flank of Mýrdalsjökull, inundating the Mýrdalssandur outwash plain before dissipating offshore [*Tómasson*, 1996] (Figure 1). Volcanogenic jökulhlaups from Katla typically begin within a few hours of the onset of the eruption. It is believed that subglacial topography does not allow floodwater to accumulate in large quantities at the eruption site [*Björnsson*, 2002]; instead, floodwater propagates rapidly from its source location toward the edge of the ice cap [*Roberts*, 2005]. Within just a few hours, the resulting jökulhlaup reaches a maximum discharge of-the-order of 100,000 m^3 s^{-1}.

[1]Nordic Volcanological Center, Institute of Earth Sciences, University of Iceland, Reykjavík, Iceland.
[2]Institute of Earth Sciences, University of Iceland, Reykjavík, Iceland.
[3]Physics Department, Icelandic Meteorological Office, Reykjavík, Iceland.
[4]LGIT-Universite de Savoie, Le Bourget du Lac Cedex, France.
[5]Department of Business and Natural Sciences, University of Akureyri, Iceland.

0148-0227/08/2006JB004851$09.00

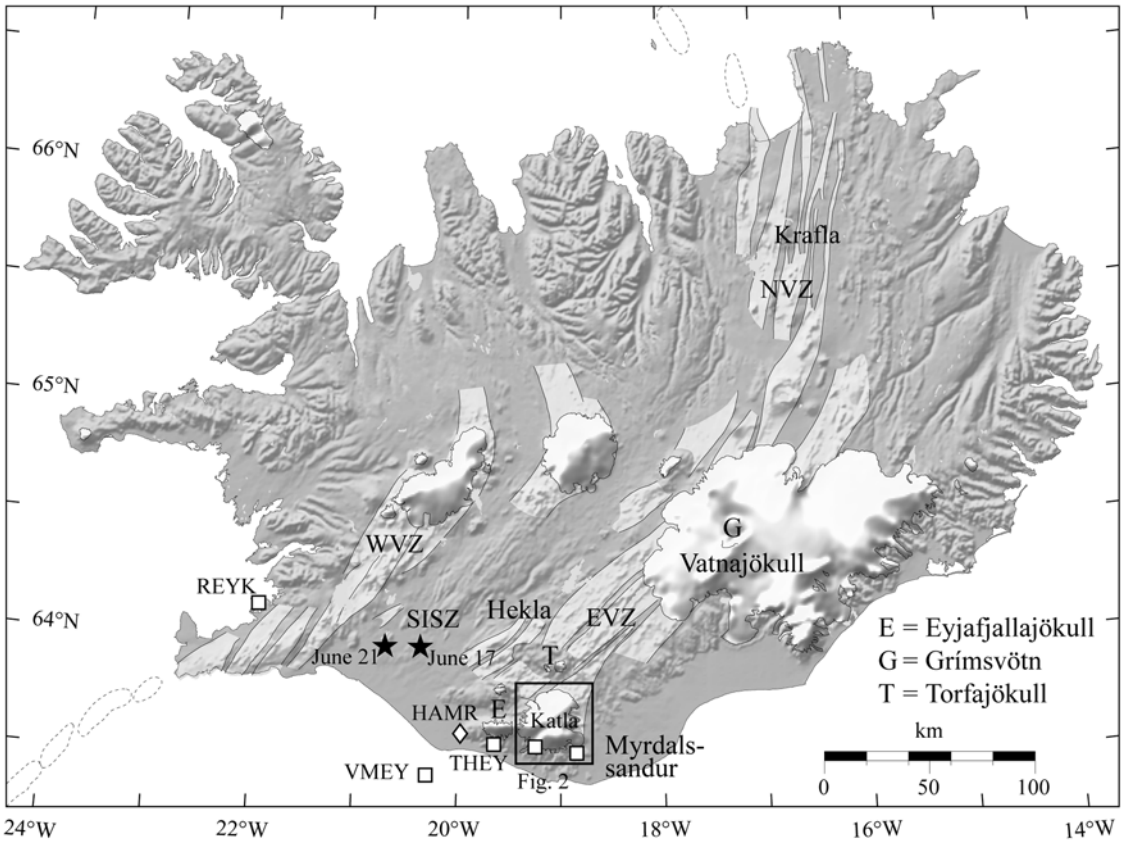

Figure 1. Map of Iceland showing the neo-volcanic zone, which is divided into the Northern Volcanic Zone (NVZ), the Western Volcanic Zone (WVZ), and the Eastern Volcanic Zone (EVZ) [*Einarsson and Sæmundsson*, 1987]. The EVZ and the WVZ are connected by the South Iceland Seismic Zone (SISZ). The stars indicate the epicenters of the two magnitude 6.6 (M_S) earthquakes on 17 and 21 June 2000. Continuous GPS stations are represented by squares and the diamond signifies the reference station (HAMR) for geodetic measurements of Katla volcano. The REYK GPS station is used as reference for the continuous stations around the Katla volcano.

[3] Iceland's national seismic and continuous GPS (CGPS) networks – maintained by the Icelandic Meteorological Office – are used to follow seismicity and crustal deformation at Katla (Figures 2 and 3). Near-real-time data from these networks are available at http://hraun.vedur.is/ja. Seismic and CGPS observations at Katla are complemented by campaign GPS surveys, optical tilt measurements, observations of ice-surface changes, and hydrological monitoring of glacial rivers from Mýrdalsjökull. In combination, these observations allow comprehensive monitoring of the changing state of the Katla volcano. In this article, we analyze the period of unrest that started in 1999 and assess the present state of the Katla volcano. For this analysis we study variations in seismicity, crustal deformation fields, and changes in the surface of the ice cap, both in relation to changes in geothermal activity and variations in ice load. The hydrological monitoring of glacial rivers is performed by the National Energy Authority and is not discussed further in this paper; for additional information see http://www.os.is.

2. Geological Background

[4] The Katla volcano hosts a 600 to 750-m deep caldera filled by ice [*Björnsson et al.*, 2000]. The caldera rim is breached in three places, to the south-east, north-west and south-west. These gaps in the caldera rim provide outflow paths for ice in the caldera to feed the main outflow glaciers, Kötlujökull, Entujökull, and Sólheimajökull (Figure 2). Apart from the large Eldgjá flood lava eruption 934-40 [*Thordarson et al.*, 2001], all historic eruptions of the Katla volcanic system have occurred within the caldera [*Larsen*, 2000]. Since the 10th century AD, all large jökulhlaups caused by Katla eruptions have emerged from Kötlujökull while large jökulhlaups issued from Sólheimajökull in the 8th and 9th centuries AD [*Elíasson et al.*, 2006]. During historical time, at least two volcanogenic jökulhlaups are known to have burst from Sólheimajökull: one during the Eldgjá eruption, the other in 1860 [*Larsen*, 2000] (Figure 2). Large, pre-historic jökulhlaups have issued from Entujökull on the north-west flank of the volcano [*Haraldsson*, 1981; *Smith*, 2004; *Smith and Dugmore*, 2006; *Larsen et al.*, 2005], and Sólheimajökull on the south-west flank, as evidenced by jökulhlaup deposits.

[5] The tectonic setting of the Katla volcano is not simple, as it is located outside the main zones of divergent plate motion. In south Iceland the plate boundary is in a state of transition [e.g., *Einarsson*, 1991a; *Sigmundsson et al.*, 1995; *Sigmundsson*, 2006]. Plate divergence is presently

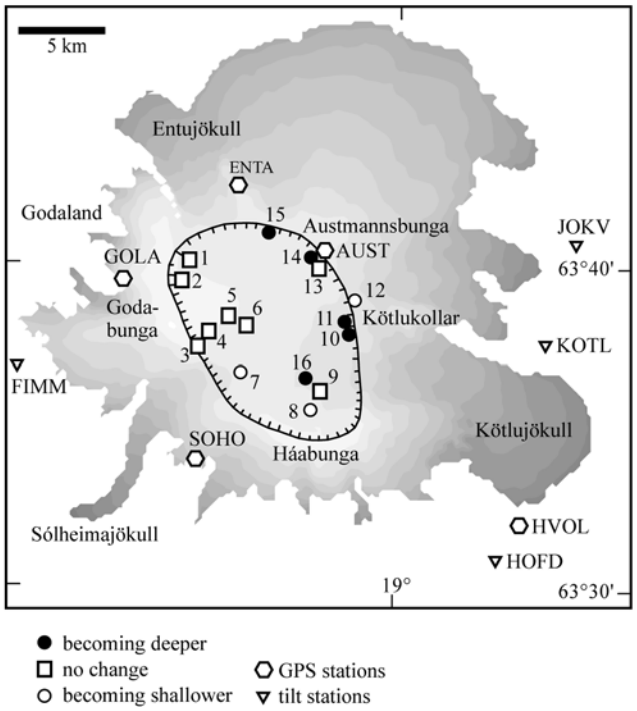

Figure 2. Schematic view of Mýrdalsjökull showing the subglacial outline of the Katla caldera and the numbered location of ice-surface depressions (cauldrons) monitored during the period 2001–2004. White circles represent cauldrons that were becoming shallower, whereas black circles indicate cauldrons that were getting deeper. White squares represent cauldrons with a fixed surface elevation during the observation period. The optical tilt stations around Mýrdalsjökull are shown in inverted triangles.

taken up by two parallel rift zones: the West Volcanic Zone (WVZ) and the East Volcanic Zone (EVZ). Latitude-dependent variations in spreading rate are observed in both zones, with the EVZ accommodating 55–100% of the relative motion between the North America and Eurasia plates [*LaFemina et al.*, 2005]. The spreading rate decreases southwards and active rifting terminates at the Torfajökull volcano (Figure 1), where the EVZ rift zone meets the transform boundary of the South Iceland Seismic Zone. From Torfajökull to the Vestmannaeyjar islands, the influence of the EVZ is primarily seen in the decreasing alkalinity of rocks with increasing distance from the tip of the rift zone [*Óskarsson et al.*, 1982]. Therefore Katla and the neighboring volcanoes Eyjafjallajökull and Vestmannaeyjar (including the Heimaey and Surtsey eruption sites) move completely with the Eurasia plate [*LaFemina et al.*, 2005; *Geirsson et al.*, 2006]. Hence Katla may be classified as an intraplate volcano, in spite of its occasional connection with rifting in the EVZ, exemplified by the AD 934 Eldgjá eruption.

[6] The volcanic products of Katla are primarily bimodal in composition, comprising alkali basalt and mildly alkalic rhyolites [*Lacasse et al.*, 2007]. Intermediate rocks, mostly basalt-rhyolite hybrids and occasional hawaiite are very subordinate [*Lacasse et al.*, 2007]. Volumetrically, FeTi-rich basalt with aphyric appearance dominates. This is ascribed to rapid segregation of material from a large mantle-source beneath a propagating rift [*Sinton et al.*, 1983]. Silicic volcanism is an important component of Katla's activity. At least 12 silicic tephra layers are known from Katla during the Holocene, between 1700 and 6600 BP. [*Larsen et al.*, 1999; *Larsen*, 2000], and almost all known outcrops of Katla at the caldera rim and immediately outside it are silicic [*Jóhannesson et al.*, 1990; *Lacasse et al.*, 2007]. Katla tephras show that phreato-magmatic eruptions have occurred throughout the Holocene [*Óladóttir et al.*, 2005].

[7] Seismic undershooting within the Katla caldera has revealed a zone where P wave velocities are reduced and S-waves are absent; this anomaly is interpreted as evidence of a magma chamber [*Gudmundsson et al.*, 1994]. Moreover, results from an aeromagnetic survey indicate the presence of a non-magnetic body within the region of the postulated magma chamber [*Jónsson and Kristjánsson*, 2000].

[8] Since 1994, the ice-capped Eyjafjallajökull volcano, situated 25 km west of Katla, has been the most active source of crustal deformation signals in the region [*Sturkell et al.*, 2003a] (Figure 1). In 1994, and again in 1999, magma intrusion was detected under the southern slopes of Eyjafjallajökull. These intrusions had a center of uplift ~4 km southeast of the volcano's summit crater [*Sturkell et al.*, 2003a; *Pedersen and Sigmundsson*, 2004, 2006] and

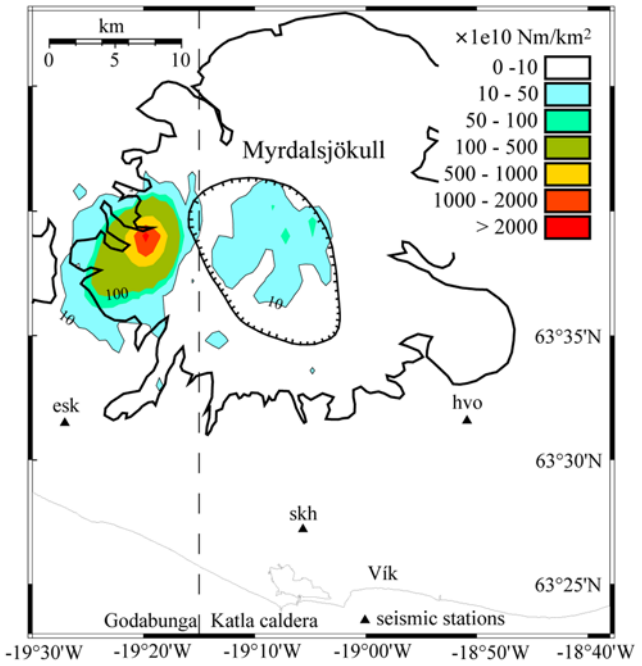

Figure 3. Earthquake activity in the Katla volcano and the location of nearby seismic stations forming part of the national seismic network. Contours depict the cumulative seismic moment per square kilometer for the period 01 January 1997 to 28 February 2005. The seismic moment was calculated using the moment-magnitude relation $\log M_0 = 1.5 M_{LW} + 9.1$, where M_0 is the moment (N m) and M_{LW} moment magnitude for earthquakes $M_{LW} \geq 1.7$. Earthquake activity is focused in two regions: the area within the Katla caldera (234 events) and the Goðabunga region (3020 events), separated by the dashed line.

were associated with considerable seismic activity [e.g., *Dahm and Brandsdóttir*, 1997]. After the intrusion event in 1999 crustal deformation and earthquake activity at Eyjafjallajökull has remained low [*Sturkell et al.*, 2006]. This is, however, not the only known case of simultaneous activity of Eyjafjallajökull and Katla. The two volcanoes apparently both erupted in 1612 and the Eyjafjallajökull eruption of 1821–23 was immediately followed by an eruption of Katla [*Thoroddsen*, 1925]. These are the only known eruptions of Eyjafjallajökull in historic times.

3. The 1918 Eruption of Katla

[9] The latest large eruption of Katla began on 12 October 1918, lasting for about three weeks [*Sveinsson*, 1919; *Jóhannsson*, 1919]. It was a basaltic eruption and the eruption site was near the southeast rim of the caldera, beneath about 400 m of ice. At 13:00 GMT, earthquakes were felt in the village of Vík (Figure 3); two hours later, an eruption column was seen over Mýrdalsjökull from Vík. At about the same time, a debris-laden jökulhlaup was seen propagating over Mýrdalssandur at a speed of about 10 m s^{-1} [*Tómasson*, 1996]. The height of the eruption plume on 12 October was estimated at 14 km a.s.l. and tephra was carried northeast [*Thorarinsson*, 1975; *Larsen*, 2000]. By 13 October, the intensity of the eruption had diminished significantly, the jökulhlaup had almost abated, and the eruption ended on 04 November. The maximum discharge of the jökulhlaup on 12 October is estimated at 300,000 m^3 s^{-1} [*Tómasson*, 1996]. The total volume of the 1918 jökulhlaup may be as high as 8 km^3 [*Tómasson*, 1996]. An enormous amount of debris was deposited in the sea, advancing the Mýrdalsssandur coastline by 3–4 km; however, this temporary extension to the coast was reduced to 2 km a few months later [*Sveinsson*, 1919]. The 1918 eruption of Katla was large, but estimates of the total volume of erupted material vary. The amount of tephra fallout is estimated at 0.7 km^3 [*Eggertsson*, 1919] and the volume of water-transported material is estimated at between 0.7 and 1.6 km^3 [*Larsen*, 2000]. The dense-rock equivalent may have been as high as 1 km^3.

4. Short-Lived Katla Eruptions in 1955 and 1999?

[10] It is possible that a short-lived subglacial eruption took place in 1955 on the eastern rim of the Katla caldera; however, no tephra erupted into the atmosphere. Instead, two shallow ice cauldrons formed in the surface of Mýrdalsjökull and a small jökulhlaup drained from Kötlujökull [*Thorarinsson*, 1975; *Rist*, 1967]. Additionally, earthquakes were detected beneath Mýrdalsjökull in the hours preceding the onset of the jökulhlaup [*Tryggvason*, 1960]. The 1955 jökulhlaup destroyed a bridge and caused damage to telecommunication lines.

[11] A similar, but possibly smaller, event took place in July 1999. Late on 17 July 1999, earthquakes and bursts of low-frequency seismic tremor were registered at seismic stations around Mýrdalsjökull [*Einarsson*, 2000; *Vogfjörð*, 2002]. This tremor sequence culminated in the release of a jökulhlaup from Sólheimajökull (Figure 2) early on 18 July [*Sigurðsson et al.*, 2000; *Roberts et al.*, 2003]. Following the jökulhlaup, a newly formed ice cauldron (Figure 2) was seen in the surface of Mýrdalsjökull [*Gudmundsson et al.*, 2007]. In the weeks following the 1999 jökulhlaup, increased geothermal activity was detected along the caldera rim, as manifest by the deepening of pre-existing ice cauldrons [*Gudmundsson et al.*, 2007]. The 1999 jökulhlaup damaged unpaved roads, electrical pylons, and it almost overtopped a bridge.

5. Seismic Unrest in 1967 and 1976–77

[12] At Katla, periods of high seismic activity were observed in 1967 and 1976–77 [*Einarsson*, 1991a]. In both cases, seismicity remained elevated for about a year. It is problematic to compare seismicity over such an extended period of rapid progress in monitoring technology. Only four seismic stations were in operation in Iceland in 1967 so no accurate locations are available for the activity. In 1976 a local network of analog stations had been installed allowing a fairly high resolution of the location of the activity [*Einarsson and Brandsdóttir*, 2000]. The different networks require different magnitude scales for the earthquakes. The largest earthquakes in Katla are detected teleseismically by stations on both sides of the Atlantic. They determine m_b (body wave magnitude) from the teleseismic P-waves and are comparable for the whole observation period. They also sometimes determine M_S (surface wave magnitude) from long wavelength Rayleigh waves, that are considered to be even more reliable as a measure of earthquake size. For smaller events the M_L-scale (local magnitude) is the most commonly used scale. M_L is determined from the maximum amplitude of the event as recorded by local seismographs. Where these magnitude scales overlap they have been found to agree well.

[13] The 1967 episode was noticed early in the year due to persistent activity that included earthquakes of m_b 4.5 and 4.1, which were recorded teleseismically (ISC). The largest earthquake, m_b 5.0 (ISC), occurred on 01 April, and dense swarms took place in April and July, with events larger than M_L 4. The largest swarm began on 03 October, lasting for 4 days; this swarm contained seven events larger than M_L 4, one of which was recorded teleseismically with an m_b of 4.5 (ISC). The locational accuracy of the 1967 activity did not allow the recognition of discrete source areas beneath the ice cap.

[14] The 1976–1977 seismic crisis was well recorded by a newly installed local seismograph network. Two epicentral areas could be identified within the Katla area, one in the caldera and the other at Goðabunga west of the caldera. Both the western and the eastern source areas contributed to the increased activity, i.e., both the caldera region and the Goðabunga cluster were active and agitated. The activity increased gradually in June, July, and August 1976, and then rather dramatically in September–November. The activity continued at a slightly diminishing rate for four months. A few events reached M_L 4. No events were detected teleseismically until 24 March 1977. Then an m_b 4.7 event occurred in the caldera region and was felt at several nearby farms. A slightly larger event occurred on 02 June (m_b 4.9; M_S 5.0) that was widely felt in the region. The fault plane solution for this event showed a large component of reverse faulting [*Einarsson*, 1987]. The

physical mechanism of the two seismicity episodes is still unclear. *Einarsson* [1991a] pointed out that both periods were preceded by eruptions in the Vestmannaeyjar volcanic system, about 60 km west of Katla.

[15] Written documents show that all large Katla eruptions since at least 1625 have been preceded by earthquakes that were felt in neighboring areas [*Thoroddsen*, 1925]. It is likely that older eruptions were also preceded by felt earthquakes, but documentary evidence is lacking. Typically the eruptions of Katla have become visible 1–8 h after the first felt earthquake [*Thorarinsson*, 1975].

6. Methods

[16] A combination of seismic and geodetic methods has been particularly successful in monitoring the state of Icelandic volcanoes [e.g., *Sturkell et al.*, 2006]. Emphasis has been put on these methods in the monitoring of Katla, but additionally the location of the volcano beneath an ice cap allows indirect monitoring of the heat flux from the volcano by observing cauldrons in the ice surface produced by melting of ice at the rock-ice interface. Mýrdalsjökull is one of the most seismically active regions in Iceland, with earthquakes occurring both within the Katla caldera and on the western flank of the volcano in the Goðabunga region (Figure 3). Local seismograph observations are available since the fifties and seismic networks of high sensitivity have been operated in the area continuously since 1973 [*Einarsson and Brandsdóttir*, 2000]. For this study we rely mainly on data from the digital SIL network installed in 1990. SIL (South Iceland Lowland) was originally a seismic network with near-real time data acquisition in south Iceland. Currently the SIL acronym refers to the whole Icelandic seismic network, which has been spread to most of the country. The network is reasonably sensitive for this region. The earthquake catalog of the Iceland Meteorological Office for the Katla area is complete for events larger than M_{Lw} 1.4 (local moment magnitude).

[17] Four optical tilt stations are installed around Mýrdalsjökull (Figure 2). Three of them were installed in 1967 by *Tryggvason* [1973] to measure ground deformation around the Katla volcano. The Jökulkvísl (JOKV) and Kötlukriki (KOTL) tilt stations are located east of Mýrdalsjökull, and the Höfðabrekkuheiði (HOFD) station to the southeast (Figure 2). An additional tilt station was installed in 1992 at Fimmvörðuháls (FIMM), situated between Mýrdalsjökull and Eyjafjallajökull (Figure 2). Station FIMM is close to the Goðabunga area, enabling monitoring of ground motion and magma movements in the western part of the volcano. Stations JOKV, KOTL, and FIMM are visited annually but station HOFD has proven unreliable, hence it is seldom visited [*Tryggvason*, 2000]. The HOFD benchmarks are set in porous tuff and have tended to come loose and give inconsistent results.

[18] Two continuously recording GPS-stations were installed in 1999 to monitor crustal deformation around Katla. These stations are Sólheimaheiði (SOHO) and Láguhvolar (HVOL), located to the south and southeast of Mýrdalsjökull, respectively (Figure 2). The Continuous GPS-network (CGPS) is complemented by campaign GPS measurements. Benchmarks on the nunataks on the caldera rim which were first measured in 1993, have been surveyed at least annually since 2000. For an overview of the GPS processing procedure [see *Sturkell et al.*, 2003a].

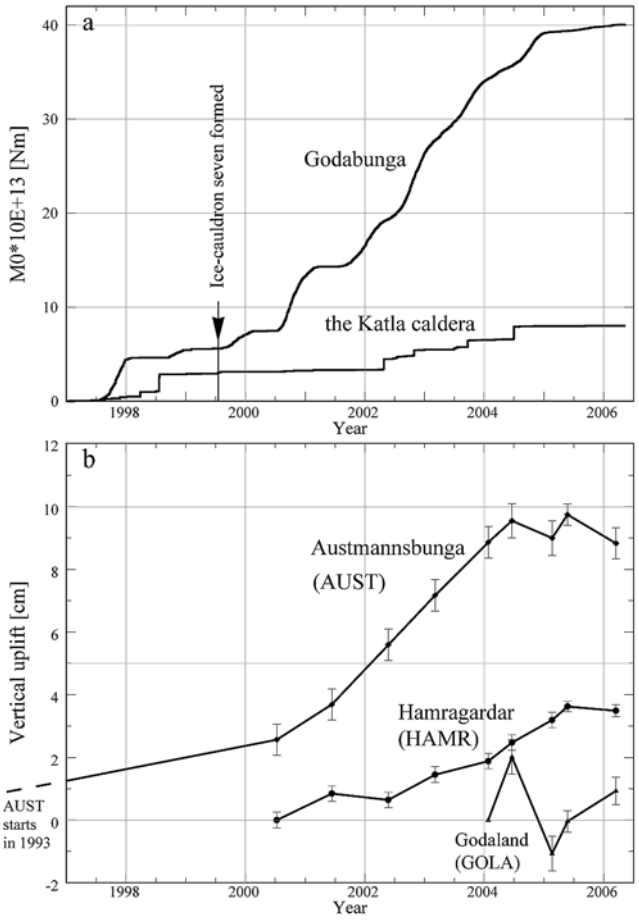

Figure 4. Time series plot of geodetic and seismic data for the Katla volcano. (a) Cumulative seismic moment for the Katla caldera and the Goðabunga region (see Figure 3 for explanation). Between 2002 and the beginning of 2005 earthquakes took place year-round within the Goðabunga region. Note that ice-cauldron seven (see Figure 2) formed before the onset of sustained earthquake activity in the Goðabunga region. (b) Vertical displacement of GPS benchmarks at Austmannsbunga (AUST), Goðaland (GOLA), and Hamragarðar (HAMR) since 1993 (see Figures 1 and 2). Displacement at AUST and GOLA is relative to HAMR, which is referenced to Reykjavík (REYK) (see Figure 1). To clarify the use of geographic names; Goðaland is a mountain range on the western flank of the Goðabunga glacier summit (1512 m.a.s.l.).

[19] Last, elevation profiles over Mýrdalsjökull were obtained using an aircraft-mounted radar altimeter whose exact position was recorded continuously using a kinematic GPS. Within the survey area, the minimum elevation accuracy of these combined measurements was ±2 m [*Gudmundsson et al.*, 2007]. A preliminary version of the altimeter system was used to monitor ice-surface subsidence during a volcanic eruption beneath Vatnajökull in 1996 [*Gudmundsson et al.*, 2004] (Figure 1). A description of the system is given by *Gudmundsson et al.* [2007]. Since October, 1999 altimeter measurements have been made

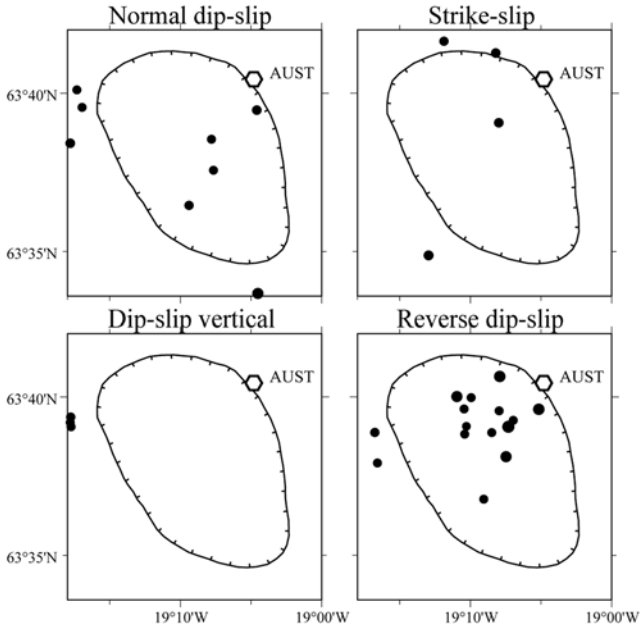

Figure 5. Earthquake epicenters within the Katla caldera for events $M_{LW} \geq 3$ during the period 1997 to 2004. Earthquakes are categorized in relation to the optimal fault plane solution for each event, as represented by the four panels.

twice a year along nine survey lines intersecting all known ice cauldrons These profiles provide the observational basis for the changes in thermal output of the geothermal areas underlying the ice cauldrons within the caldera [*Gudmundsson et al.*, 2007] as well as shrinkage of the ice cap due to climate warming which is mostly manifested by retreat of outlet glaciers [*Pinel et al.*, 2007].

7. Seismic Observations

[20] Since at least 1960, seasonal earthquake activity has occurred beneath Goðabunga, with earthquakes typically beginning in early autumn, peaking in late autumn, and continuing until mid-winter [*Einarsson and Brandsdóttir*, 2000; *Jónsdóttir et al.*, 2007]. However, in early 2002 earthquake activity did not stop; instead, sustained activity was maintained throughout the year (Figure 4a). Persistent earthquake activity was observed beneath Goðabunga until late 2004. The seasonal correlation was still noticeable, but the activity did not stop in the winter as it typically did before 2002. In early 2005 the earthquake activity again diminished substantially (Figure 4a). It is noteworthy, however, that in spite of the lower level the activity never stopped completely during the winters of 2005 and 2006. From 1997 to 2004, the largest earthquake beneath Goðabunga registered M_{LW} 2.8.

[21] During the period of our study the seismicity within the Katla caldera has been considerably lower than around Goðabunga. Seasonal correlation is less pronounced for these earthquakes (Figure 4a) [*Jónsdóttir et al.*, 2007]. The largest earthquakes in the Mýrdalsjökull region originate in the northeast part of the Katla caldera, and since 1997 earthquakes up to M_{LW} 3.6 have occurred there. This indicates that the magnitude-frequency distribution for the

Table 1. Horizontal and Vertical Displacements and Tilt Calculated for the Most Frequently Measured Sites on and Around Katla, Modeled as the Result of Point Pressure Source at the Depth d (Mogi Model)[a]

(a) Inflation Center Within the Caldera		x [m] 593,000	y [m] 7060,000	h_0 [m] 0.12	d [m] 4900
Name		Dist., m	Vert., cm	Hz., cm	Tilt, μrad
Austmannsbunga	AUST	3,053	7.34	4.57	20.16
Enta	ENTA	6,044	3.00	3.70	8.98
Fimmvörðuháls	FIMM	16,532	0.28	0.93	0.46
Goðaland	GOLA	9,941	1.04	2.10	2.52
Hamragarðar	HAMR	42,951	0.02	0.15	0.01
Höfðabrekkuheiði	HOFD	20,359	0.15	0.64	0.21
Jökulkvísl	JOKV	17,327	0.24	0.86	0.39
Kötlukriki	KOTL	15,201	0.35	1.08	0.62
Láguhvolar-FS	HVOL	19,691	0.17	0.68	0.24
Sólheimaheiði-FS	SOHO	12,897	0.54	1.42	1.09
Vestmannaeyjar	VMEY	63,514	0.01	0.07	0.00
(b) Goðabunga		x [m] 582,513 Dist., m	y [m] 7060,798 Vert., cm	h_0 [m] 0.31 Hz., cm	d [m] 2000 Tilt, μrad
Austmannsbunga	AUST	12,551	0.01	0.08	0.03
Enta	ENTA	8,540	0.04	0.16	0.12
Fimmvörðuháls	FIMM	8,247	0.04	0.17	0.14
Goðaland	GOLA	703	2.60	0.92	12.22
Hamragarðar	HAMR	32,659	0.00	0.01	0.00
Höfðabrekkuheiði	HOFD	28,649	0.00	0.01	0.00
Jökulkvísl	JOKV	27,605	0.00	0.02	0.00
Kötlukriki	KOTL	25,683	0.00	0.02	0.00
Láguhvolar-FS	HVOL	28,550	0.00	0.02	0.00
Sólheimaheiði-FS	SOHO	13,118	0.01	0.07	0.02
Vestmannaeyjar	VMEY	54,551	0.00	0.00	0.00

[a]Locations are listed in UTM co-ordinates (zone 27). (a) Expected displacements caused by an inflating point-source in the Katla caldera for a four-year period (inflation rate h_0 = 3.0 cm y^{-1}). Note that deformation signals are small beyond 15 km distance. (b) Deformation caused by the ascent of the hypothesized cryptodome beneath Goðaland from January 2004 to June 2004. The location and depth of the cryptodome is deduced from earthquake distributions [*Soosalu et al.*, 2006], and measured GPS displacements at GOLA are fitted to a point source, which equates to 3.1 cm of vertical uplift (h_0). Signals are small everywhere else.

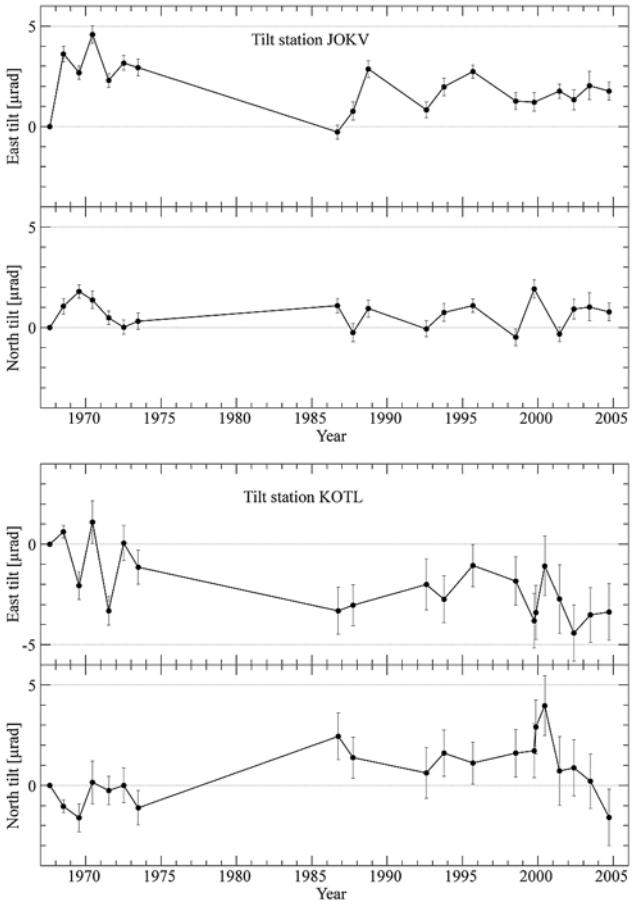

Figure 6. Observed ground tilt at the Kötlukriki (KOTL) and Jökulkvísl (JOKV) leveling stations, located on the eastern flank of the Katla volcano (see Figure 2). At both sites, the eastward component exhibits alternating uplift and subsidence between 1967 and 1973. This has been interpreted as the effect of annual variations in ice load [*Tryggvason*, 2000]. More recently, this trend is less obvious in the tilt data. At the Kötlukriki station, the downward trend in the north component from 2001 onwards is probably due to thinning of the nearby glacier Kötlujökull.

two populations of earthquakes, Goðabunga and caldera earthquakes, is different. Within the caldera, the optimal fault plane solution [*Rögnvaldsson and Slunga*, 1993] for the majority of earthquakes greater than M_{LW} 3 shows reverse faulting (Figure 5).

8. Tilt Measurements

[22] Both in 1994 and 1999 tilt measurements at station FIMM revealed crustal uplift toward the southern flank of Eyjafjallajökull, as confirmed by GPS observations [*Sturkell et al.*, 2003a]. These episodes of uplift were interpreted as being caused by magma intrusions. At the tilt station FIMM no deformation has been detected that can be attributed to the activity at Goðabunga, which is located 8 km northeast (Table 1). The deformation field causing earthquakes at Goðabunga must therefore either be very small or very localized.

[23] From 1967 to 1973 tilt stations KOTL and JOKV, located east of Mýrdalsjökull, exhibited repeated, small uplift and subsidence (Figure 6), which *Tryggvason* [1973, 2000] attributed to annual variations in the mass of the ice cap. The observations were discontinued in 1975, mainly due to the Krafla volcano-tectonic episode (1975–1984) in N-Iceland, that was keeping the Icelandic geoscience community very busy. After tilt measurements were resumed in 1986 the cyclic pattern of uplift and subsidence was not observed, possibly due to shrinkage of the ice cap. The north component of tilt measurements made at KOTL since 2000 (Figure 6) show subsidence to the north (or uplift to the south), which might be caused by recent thinning [*Sigurðsson*, 2003] of the Kötlujökull outlet glacier, located immediately south of the measurement point.

9. GPS Measurements

[24] Using geodetic methods for monitoring volcanoes in Iceland it is important to take into account that the measured signal is superimposed on several other signals, many of which are of geodynamic importance [e.g., *Einarsson et al.*, 2006]. So in order to isolate the volcanic processes due to Katla one has to consider processes such as plate movements, plate boundary deformation, activity in neighboring volcanoes, changes in ice load etc. For our purposes it is of great importance that Katla is not located directly on the plate boundary and is only moderately influenced by events there. It is also important to note that intrusion events took place in the neighboring Eyjafjallajökull in 1994 and 1999. These events did have a measurable effect in our network.

[25] All campaign measurements presented here use the Hamragarðar (HAMR) benchmark as fixed in the processing. The displacement relative to the fixed HAMR for the different surveys are given in Table 2. Some data from CGPS stations are included in campaign measurements, but long-term observations are processed relative to station REYK, located in Reykjavík (Figure 1). Although HAMR is located outside the deformation field created by Katla, the intrusion event of 1999 beneath the neighboring Eyjafjallajökull volcano caused 1.0 cm of westward displacement (Figure 7) and the 1994 event that was very similar, probably did so as well. Additionally, in June 2000, two M_S 6.6 earthquakes struck in southern Iceland (Figure 1). Both of these earthquakes were produced by right-lateral slip on N–S trending faults; the resulting crustal deformation was detected clearly at HAMR [*Sturkell et al.*, 2003a] (Figure 7). In addition, it is apparent that REYK is subsiding at a rate of 0.3 cm a^{-1} [*Geirsson et al.*, 2006]. However, this anomaly is not taken into account in data from HAMR and SOHO.

[26] In comparison to the NUVEL-1A plate model, station SOHO (and to some extent HVOL) shows accelerating southward displacement since mid 2000, which we attribute to a local source (Figure 8). Relative to REYK, the vertical signal from SOHO varies annually, but the overall trend between mid 2000 and 2005 is vertical uplift at a rate of about 1 cm a^{-1}. The same annual cycle has been observed at several nearby CGPS stations but with varying amplitudes [*Geirsson et al.*, 2006; *Grapenthin et al.*, 2006].

[27] From 2001 until 2004 constant uplift at AUST occurred at a rate of 1.8 cm a^{-1} (Figure 4b). Figure 9

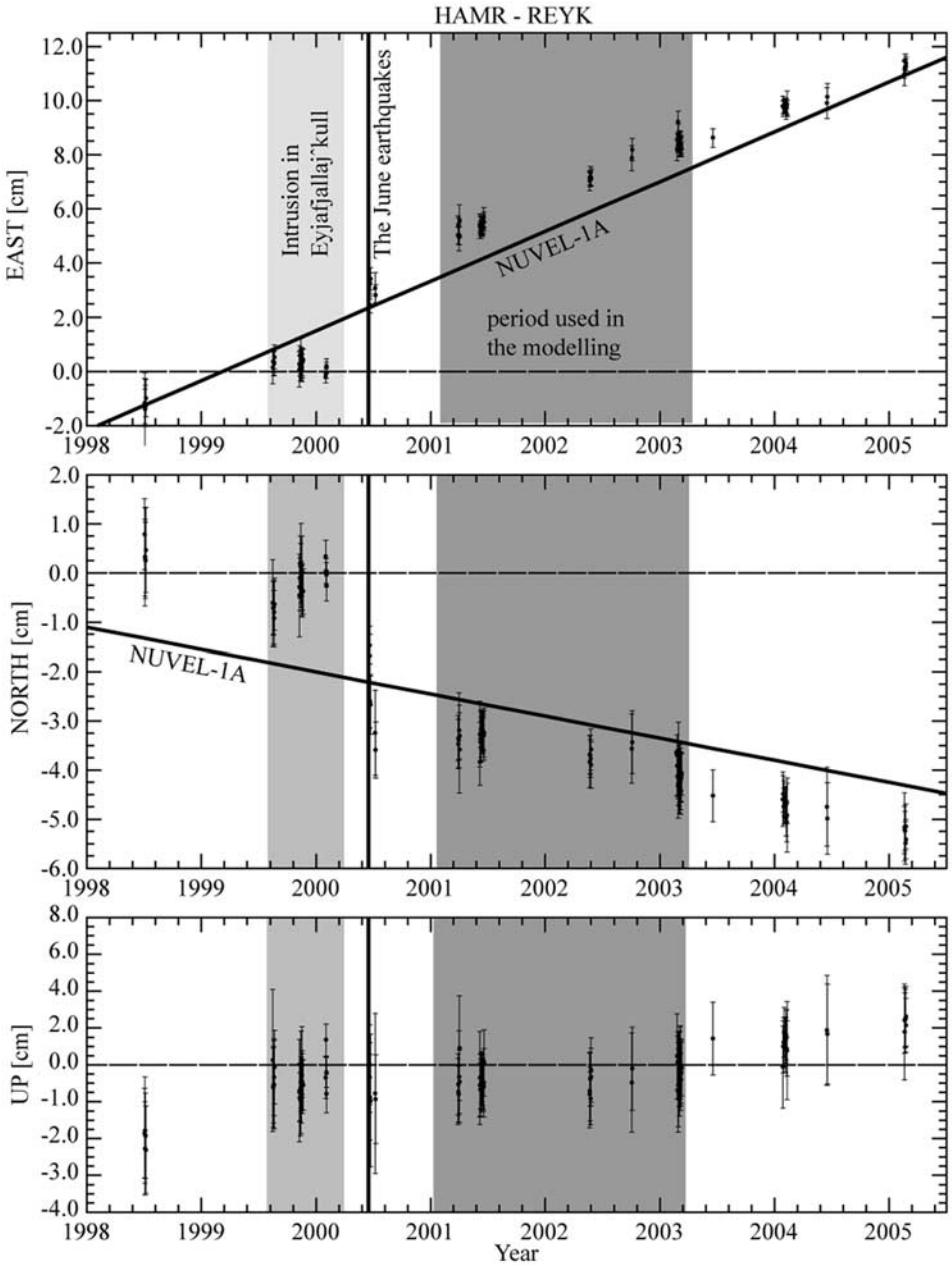

Figure 7. Time-series plot of displacement at HAMR relative to REYK station, which was held fixed during data processing. The solid lines in the east and north component show the predicted movement of the station according to the NUVEL1-A model of plate motion [*DeMets et al.*, 1994]. An intrusion event at Eyjafjallajökull caused westward movement of HAMR relative to the NUVEL1-A model. Horizontal motion was also affected by two major strike-slip earthquakes, which occurred in the SISZ in 2000 (see Figure 1). No vertical displacement was detected at HAMR as a consequence of the 2000 earthquakes. Following the earthquakes, however, progressive uplift has occurred.

shows the derived displacement vectors from benchmarks on and around Mýrdalsjökull, relative to HAMR. Between March 2003 and January 2004 (Figure 9b), vertical uplift and radial displacement from the caldera center was observed, except for one measurement from AUST, which exhibited horizontal displacement toward the caldera center (Figure 9b). The probable reason for the apparent inward movement of AUST is earthquake activity in August 2003 that originated in the northeast sector of the caldera, very close to the station (Figure 5).

[28] In an attempt to monitor crustal deformation in the zone of maximum earthquake activity in the Goðabunga region (Figure 3), we installed a GPS benchmark (GOLA) in 2004 to the immediate west of the ice cap (Figure 9d). Within a six-month interval, 2.0 cm of uplift was detected at GOLA (Figure 4b). Observations spanning the period June 2004 to February 2005 revealed the same magnitude of subsidence at GOLA, in tandem with 0.5 cm of subsidence at AUST (Figure 4b). Collectively, the GPS data demon-

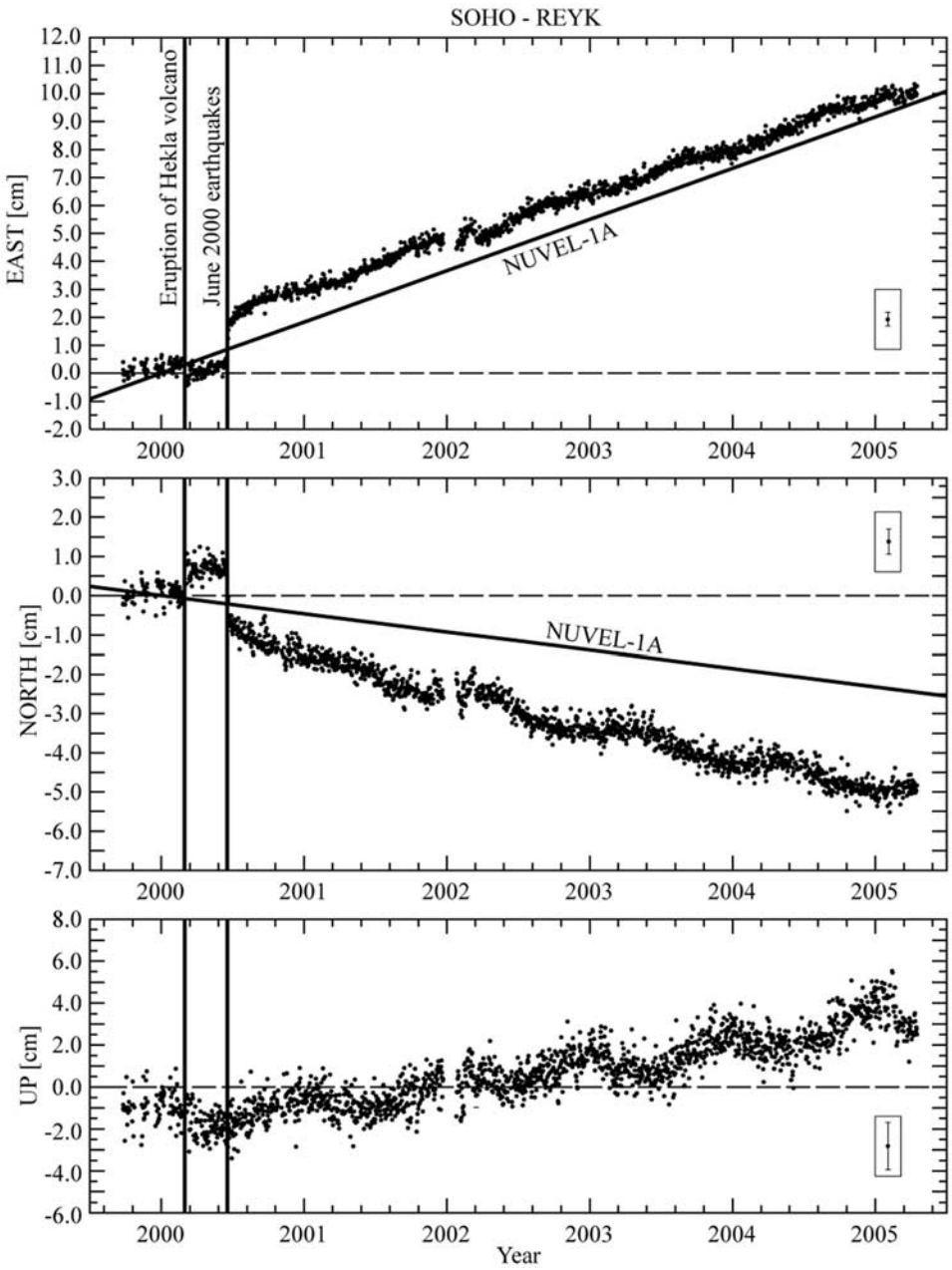

Figure 8. Time-series plot of displacement at SOHO relative to REYK, which was held fixed during data processing. The boxed error bar illustrates the minimum accuracy. The vertical lines denote the timing of the Hekla volcanic eruption in February 2000 and the June 2000 earthquake sequence in southern Iceland (see Figure 1). The sloping lines indicate the predicted movement of SOHO according to the NUVEL1-A model of plate motion [*DeMets et al.*, 1994]. Since at least the June 2000 earthquakes, data in the north component display increasing southward movement relative to the NUVEL1-A model. Data in the vertical component show repeated, annual variations, superimposed on progressively increasing uplift throughout the observation period. It is suggested that variations in ice load dominate the uplift signal at SOHO, thus masking any volcanic influence.

strate sustained inflation of Katla volcano since at least 2000, culminating in 2004.

10. Ice Cauldrons and Geothermal Activity

[29] Geothermal activity within the Katla caldera is manifest by 12–17 ice cauldrons, most of which are 10–40 m deep and 0.6–1.6 km wide (Figure 2). Within the caldera accumulation of winter snow of 8–12 m (equivalent to 5–7 m of water) occurs between October and May. During the melt season (June-August) ablation removes 2–3 m (w.e.) [*Gudmundsson et al.*, 2007]. This results in positive mass balance of 2–4 m (w.e.) within the caldera. This ice is mostly transported by ice flow down the outlet glaciers. However, roughly one tenth is melted beneath the ice cauldrons that are considered to have a combined thermal

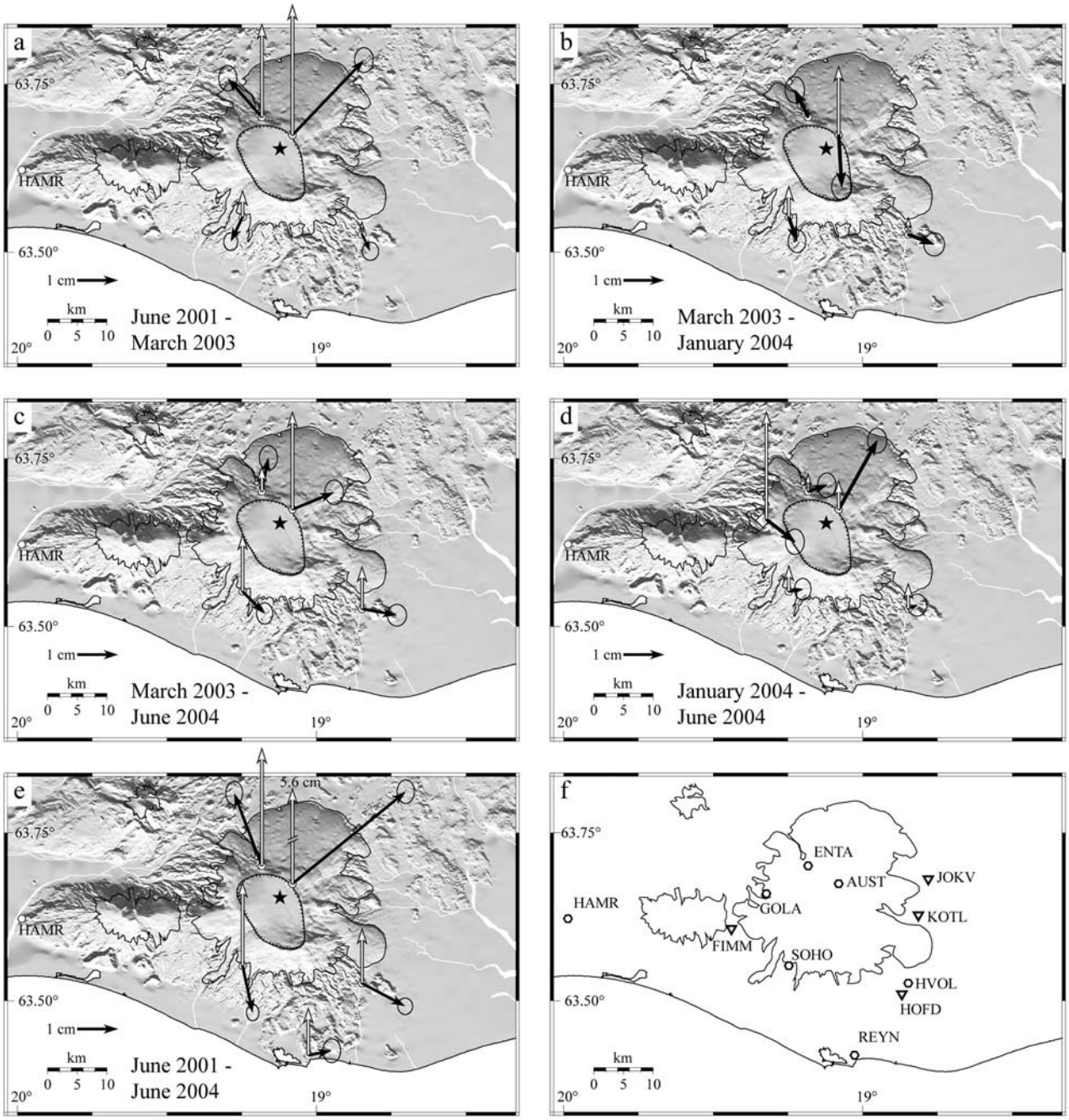

Figure 9. Displacement vectors at Katla volcano, as derived from GPS measurements between 2001 and 2004, the data are given in Table 2. Observations are relative to HAMR. The black arrows signify horizontal motion and the white arrows denote vertical movement. (a) Benchmark displacements during the period June 2001 to March 2003. These data were used to derive the best fitting point source (illustrated by a star) for the observed displacement signals. (b) Benchmark displacements during the period March 2003 to January 2004. During this period, all displacement vectors fit to the point-source model apart from the horizontal component of AUST; this behavior may be due to earthquake activity near the benchmark in August 2003 (see Figures 3 and 5b). (c) Benchmark displacements during the period March 2003 to June 2004 showing increased eastward displacement due to westward movement of HAMR (see east component of Figure 6). (d) Benchmark displacements during the period January 2004 to June 2004, encompassing the period of uplift observed at GOLA. (e) Total benchmark displacements around Katla volcano between June 2001 and June 2004. (f) Schematic view of Mýralsjökull and the Katla caldera showing the location of GPS benchmarks in Figures 9a to 9e. The optical tilt stations around Mýrdalsjökull are shown in inverted triangles.

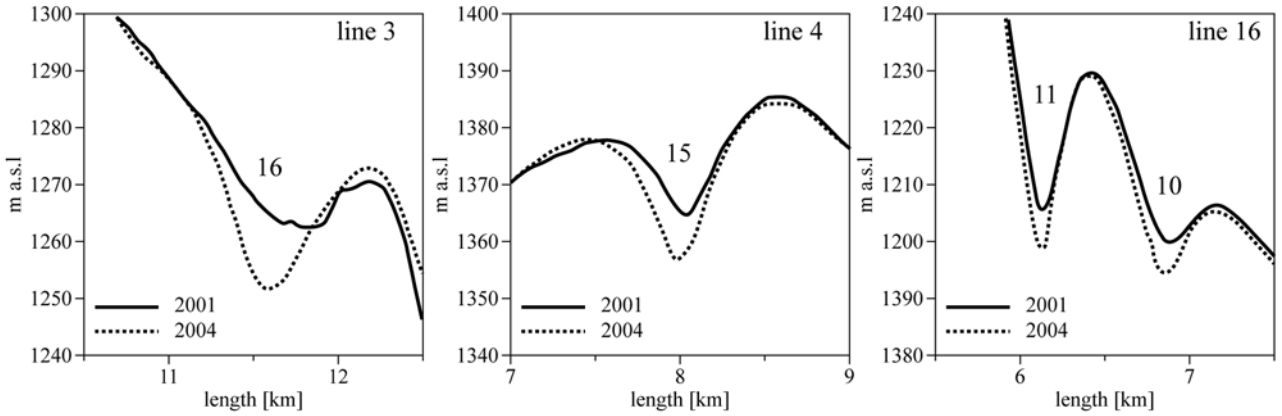

Figure 10. Radar altimeter profiles across ice cauldron 10, 11, 15, and 16 in fall 2001 and 2004. The depth of these cauldrons increased by 6–13 m over this period. Changes in the depth of other cauldrons were smaller over this period.

output of a few hundred megawatts [*Gudmundsson et al.*, 2007]. During the melt season, some cauldrons deepen considerably, signifying the release of water from storage at the glacier base beneath the site of the cauldron. The resulting jökulhlaup are manifest by increasing discharge and heightened levels of dissolved solutes in the affected river [e.g., *Sigurðsson et al.*, 2000]. The ice cauldron that formed in July 1999 (cauldron 7; Figure 2) corresponded to 20×10^6 m^3 of meltwater production, which resulted in a jökulhlaup from Sólheimajökull on 18 July [*Sigurðsson et al.*, 2000; *Roberts et al.*, 2003]. When inspected from the air at 10:00 GMT on 18 July, the newly formed cauldron had a width of 1–1.5 km and a depth of 40–50 m. Four weeks later, other ice cauldrons on the surface of Mýrdalsjökull had deepened by 5–10 m and two additional cauldrons formed: cauldrons 8 and 15 (Figure 2). Between late 1999 and mid 2001, most ice cauldrons remained at a constant depth or became shallower; however, between 2001 and 2003, the depth of cauldrons 10, 15, and 16 increased by 6–15 m. If the three year period 2001–2004 is considered, the increase also includes cauldrons 11 and 14 (Figure 2). In addition, by 2005 cauldrons 1, 2, and 5 had deepened by 5–10 m while cauldrons 10, 15 and 16 had started to decrease again [*Gudmundsson et al.*, 2007]. Figure 10 shows the change in cauldron geometry for cauldrons 10, 11, 15, and 16 between 2001 and 2004. With the exception of cauldrons 1 and 2 which are at the western caldera rim, the affected cauldrons are located on a circle with a 6–8 km radius, surrounding the northeast sector of the caldera, the region where the largest earthquakes have happened (Figures 2 and 5). This change is consistent with increased geothermal activity over the inflation bulge. The sudden appearance and then gradual decrease in the depth of cauldron 7 indicate that it was formed by a short-lived thermal pulse, such as would be produced by a small-volume, subglacial eruption.

11. Modeling of GPS Results

[30] Given that GPS measurements at HAMR were influenced by the June 2000 earthquake sequence, we included only data from June 2001 to March 2003 (Figures 7 and 11a) in a forward model designed to locate the center of the deformation source. Data from CGPS stations HVOL and SOHO, together with survey results from AUST and ENTA, yielded four three-component displacements ($n = 12$) for use in the grid search. We used a Mogi-point pressure model to calculate the best fitting location of a point-source within a grid comprising latitude, longitude, maximum uplift, and source depth. A least squares criterion was employed to minimize the χ^2 merit function [see *Bevington*, 1969].

$$\chi^2 = \sum_{i=1}^{n} \frac{res_i}{\sigma_i}. \quad (1)$$

[31] Where res_i is the residual between observations i and the model prediction, and σ_i is the standard deviation of observation i. Because of the effect of variation in ice load on vertical displacements (see separate section) we weighted the vertical component down to ensure that the effects of horizontal displacements dominated the modeling result. Figures 9 and 11 illustrate the optimal location of the point source at a depth of 4.9 km. A comparison was made by testing the model prediction against GPS data collected between June 2001 and June 2004 (Figure 11b); in this test, the residual vectors trended uniformly east with equal strength. Given the uniform size and direction of the residual vectors, we propose that slight, westward displacement of the reference station has occurred. The source responsible for this signal lies somewhere between HAMR and the measured benchmarks, with Eyjafjallajökull as the likely candidate. Mismatch between the predicted uplift value of 0.14 cm a^{-1} (Table 1) at SOHO and the observed, albeit uncorrected, value of 1 cm a^{-1} (Figure 8) suggests that non-volcanic processes are contributing to the uplift of Mýrdalsjökull.

12. Goðabunga Region: Signs of a Cryptodome?

[32] Seismicity at Goðabunga is remarkably regular, persistent, and spatially concentrated. Precise hypocentral locations reveal a zone of seismicity at 1.5 km depth [*Soosalu et al.*, 2006]. The displacement field associated with the earthquakes appears to be very localized; it is not detected at a tilt station 8 km away and apart from GOLA, none of the GPS benchmarks are affected (Table 1b). The

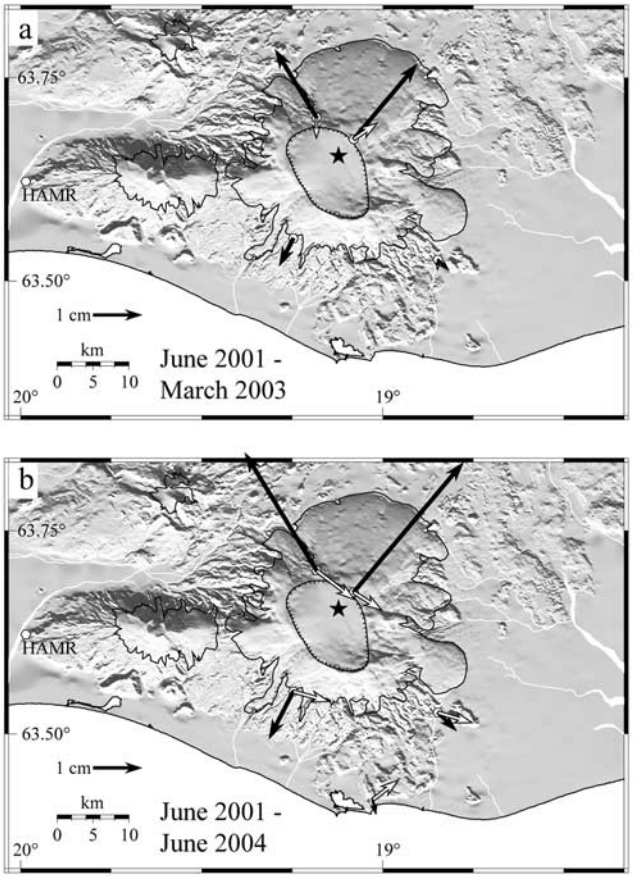

Figure 11. Total horizontal displacements and derived residual values from a point-source model of magma chamber inflation, depicted by the star. Black arrows signify measured displacement and white arrows indicate the deviation between data and model. (a) Total displacement for the period June 2001 to March 2003. The modeled point-source for the displacement signal lies at 4.9 km depth and an uplift rate of 3.0 cm a^{-1} is invoked to account for the measurements. Note that the reference benchmark (HAMR) moved at a uniform rate throughout the observation period (see Figure 6). (b) Application of the point-source model to the period June 2001 to June 2004. The uniform eastward orientation of the modeled residuals suggests westward movement of HAMR.

seasonal trend in earthquake activity in the Goðabunga region has been interpreted by *Einarsson and Brandsdóttir* [2000] as a triggering effect due to increased groundwater pressure within the volcano during summertime melting of the overlying ice cap. More recently, *Einarsson et al.* [2005] and *Soosalu et al.* [2006] have proposed that persistent earthquakes in the Goðabunga region are generated by an intruding cryptodome; that is, an ascending pocket of silicic or intermediate magma at shallow depth. This argument is based on the nature and style of the earthquake activity, the apparent displacement field, and the geographic proximity to the Katla caldera. Almost all outcrops of Katla rocks that are close to or immediately outside the caldera rim are silicic. Our deformation data are not inconsistent with this interpretation. A shallow source of pressure increase at Goðabunga will only produce small displacements and tilt at our stations (Table 1b). Furthermore, if the cryptodome is ascending without a volume increase the displacements would be smaller still.

13. Crustal Deformation Due to Variations in Ice Load

[33] An additional, alternative explanation for the observed deformation of Katla volcano is crustal rebound due to thinning of the Mýrdalsjökull ice cap. During the last decade, significant ablation of the ice cap has occurred, with radar altimeter measurements between 1999 and 2004 indicating the loss of over 3 km^3 of ice, primarily from the margins of the ice cap [*Pinel et al.*, 2007]. Would such a reduction in ice load enhance rates of crustal deformation beneath and around Mýrdalsjökull?

[34] Using GPS measurements of horizontal and vertical displacement, the influence of a changing ice-load can be assessed. Beneath and at the edge of an ice cap, vertical uplift dominates as the crustal response to ice loss, with horizontal displacements an order-of-magnitude less (ratio: <0.3) [*Pinel et al.*, 2007]; this applies to both the immediate elastic response and to the final, relaxed state of the crust. For a point-source approximation of a magma chamber, the ratio between horizontal and vertical displacement is >0.5 at distances >0.5 D, where D is the depth to the source. For Katla *Pinel et al.* [2007] showed that the derived ratio nears 1. Furthermore, the rate of horizontal displacement is 1–2 cm a^{-1} away from the caldera edge, implying that observed horizontal deformation is principally due to magma accumulation. However, some of the vertical component of displacement observed outside the ice cap may be due to glacio-isostatic response (Figure 8).

14. Ice-Cauldron Size and Geothermal Power Output

[35] The change in ice cauldron size over a three year period (2001 to 2004) can be considered to estimate the change in geothermal power output. Taking the combined additional melting (ΔV) over the three year period 2001–2004 of 1×10^7 m^3 of ice in cauldrons 10, 11, 14, 15, and 16 (Table 3), using latent-heat (L_i) and ice density (ρ_i) values of 3.35×10^5 J kg^{-1} and 910 kg m^{-3}, respectively, a minimum estimate of the increase in geothermal power (ΔP) from Katla can be obtained from: $\Delta P = \Delta V \rho_i L_i / t$. Since t is 3 years, then ΔP = 34 MW. By taking into account a likely increase of 15–50% due to increased flow of ice into an expanding cauldron [*Jarosch and Gudmundsson*, 2007] the best estimate is ΔP = 40–50 MW. Since the total power-output of the Katla volcano is considered to be a few hundred megawatts, the increased melting at the base of the Mýrdalsjökull ice cap during 2001 to 2004 may signal a 10–25% increase in geothermal heat production.

15. Insights Provided by Seismic, Geodetic, and Glaciological Observations

[36] By uniting observations presented here, together with information about previous episodes of unrest at Katla, a picture of magma accumulation since 1999 emerges. From

Table 2. All Campaign Measurements are Processed With the Hamragarðar (HAMR) Benchmark as Fixed[a]

			East, cm	Formal Uncert., cm	North, cm	Formal Uncert., cm	Up, cm	Formal Uncert., cm
(a) 01 Jun – 03 Mar								
HVOL	−18.8475	63.52632	0.203	0.007	−0.409	0.007	0.303	0.041
SOHO	−19.2466	63.55252	−0.294	0.006	−0.606	0.007	0.647	0.041
VMEY	−20.2935	63.42703	0.033	0.006	−0.108	0.008	−0.605	0.045
AUST	−19.0805	63.67440	1.756	0.007	1.840	0.010	3.184	0.057
ENTA	−19.1822	63.70112	−0.837	0.007	0.954	0.010	2.273	0.058
(b) 03 Mar – 04 Jan								
VMEY	−20.2935	63.42703	0.145	0.007	0.401	0.010	0.259	0.054
HVOL	−18.8475	63.52632	0.634	0.008	−0.240	0.009	0.409	0.052
SOHO	−19.2466	63.55252	0.197	0.007	−0.592	0.009	0.751	0.052
AUST	−19.0805	63.67440	0.076	0.008	−1.264	0.010	1.676	0.059
ENTA	−19.1822	63.70112	−0.327	0.008	0.670	0.010	0.181	0.059
(c) 03 Mar – 04 Jun								
VMEY	−20.2935	63.42703	0.642	0.006	0.590	0.009	0.880	0.050
HVOL	−18.8475	63.52632	0.854	0.008	−0.154	0.009	1.025	0.049
SOHO	−19.2466	63.55252	0.539	0.006	−0.543	0.009	1.386	0.048
AUST	−19.0805	63.67440	1.024	0.007	0.421	0.010	2.381	0.054
ENTA	−19.1822	63.70112	0.158	0.007	0.828	0.010	0.605	0.054
(d) 04 Jan – 04 Jun								
VMEY	−20.2935	63.42703	0.496	0.006	0.189	0.009	0.621	0.050
HVOL	−18.8475	63.52632	0.217	0.008	0.095	0.009	0.612	0.049
SOHO	−19.2466	63.55252	0.338	0.007	0.053	0.009	0.621	0.049
AUST	−19.0805	63.67440	0.945	0.008	1.689	0.010	0.692	0.056
ENTA	−19.1822	63.70112	0.455	0.007	0.155	0.010	0.423	0.056
GOLA	−19.3221	63.65974	0.700	0.007	−0.550	0.010	2.628	0.057
(e) 01 Jun – 04 Jun								
HVOL	−18.8475	63.52632	1.058	0.006	−0.563	0.007	1.328	0.037
SOHO	−19.2466	63.55252	0.245	0.005	−1.149	0.007	2.032	0.037
VMEY	−20.2935	63.42703	0.675	0.005	0.481	0.007	0.275	0.040
AUST	−19.0805	63.67440	2.780	0.007	2.261	0.009	5.565	0.054
ENTA	−19.1822	63.70112	−0.679	0.007	1.781	0.009	2.878	0.055
REYN	−19.0272	63.41851	0.574	0.007	0.114	0.010	1.149	0.054

[a]The displacement relative to HAMR for five different surveys combinations are given. The formal uncertainties are underestimated by the Bernese processing software [*Hugentobler et al.*, 2001] and need to be rescaled to obtain a more rigorous uncertainty estimate. Comparing the formal uncertainty to the standard deviation of the resulting coordinates scales the uncertainties.

the combined data-set it is apparent that the latest period of unrest began in July 1999 with fleeting volcanic tremor, followed immediately by a jökulhlaup from Sólheimajökull. Back-tracing the uplift curve derived from GPS measurements since 2000 (Figure 4b) we conclude that the latest episode of inflation began in mid 1999. Furthermore, our seismic and geodetic measurements confirm that, by late 2004, the inferred rate of magma accumulation had decreased significantly. Our seismic and glaciological datasets show that the largest earthquakes and the greatest concentration of deepening cauldrons occur in the northeast sector of the Katla caldera. Within the Katla caldera, between 1997 and 2004, over half of the 93 recorded earthquakes greater than M_{LW} 3 were confined to the northern part of the caldera (see Figure 5). Significantly, these earthquakes exhibited reserve, dip-slip faulting, and so too did the largest earthquake (M_{LW} 3.6). Such a dominant fault-mechanism in that region of the caldera could be explained by thrust-faulting due to crustal uplift. Likewise, the largest GPS-derived displacements have been observed at AUST on the northeast rim of the caldera (Figure 9e); nevertheless, some displacement in the vicinity of AUST may be a consequence of faulting near to the apex of the inflation bulge, as shown by earthquakes (e.g., Figure 9b). The shape of the inflation bulge is not very sensitive to the shape of the intrusive body [*Dieterich and Decker*, 1975]. As a general rule, however, the flatter the source the more pronounced will be the vertical component of displacement. The significant horizontal motion observed at Katla would therefore point to a spherical or a stock-like body rather than a flat, sill-like body. In remainder of this section, we use our geodetic results to locate the area of maximum crustal uplift and the volume of magma accumulated since 1999.

[37] The grid search for the best fitting point-source using data from June 2001 to March 2003 (1.7 years) suggests that the center of crustal uplift is located within the northeast part of the caldera at 4.9 km depth (Figure 11). However, since the contribution to vertical uplift from the reduction of ice load is not considered, this value is an overestimate. The depth may be only 2–3 km. The modeled uplift directly above the point-source is 5.1 cm for the observation period (i.e., 3.0 cm a^{-1}). Between 2000 and 2004, the surface of the volcano inflated by 0.018 km^3, as derived from the formula: $\Delta V_e = 2\pi h_0 d^2$, where h_0 corresponds to 12 cm of uplift and d represents 4.9 km depth (see Table 1a). Assuming a Poisson ratio of 0.25, the equivalent volume increase at depth is about two-thirds of the integrated surface volume; that is 0.012 km^3. In comparison, the 1918 eruption of Katla produced approximately 1 km^3 of eruptives; however, it is possible that this material was partly or solely coming from a deeper source. The relatively homogeneous chemical composition of the products of large basaltic eruptions of Katla during the last 1000 years seems to indicate that they have not had time to evolve in a shallow magma chamber [*Óladóttir et al.*, 2005, 2008]. The wide range of composition for Katla magmas in general [*Lacasse et al.*, 2007], however, points to a complicated magma plumbing system, that may even change signifi-

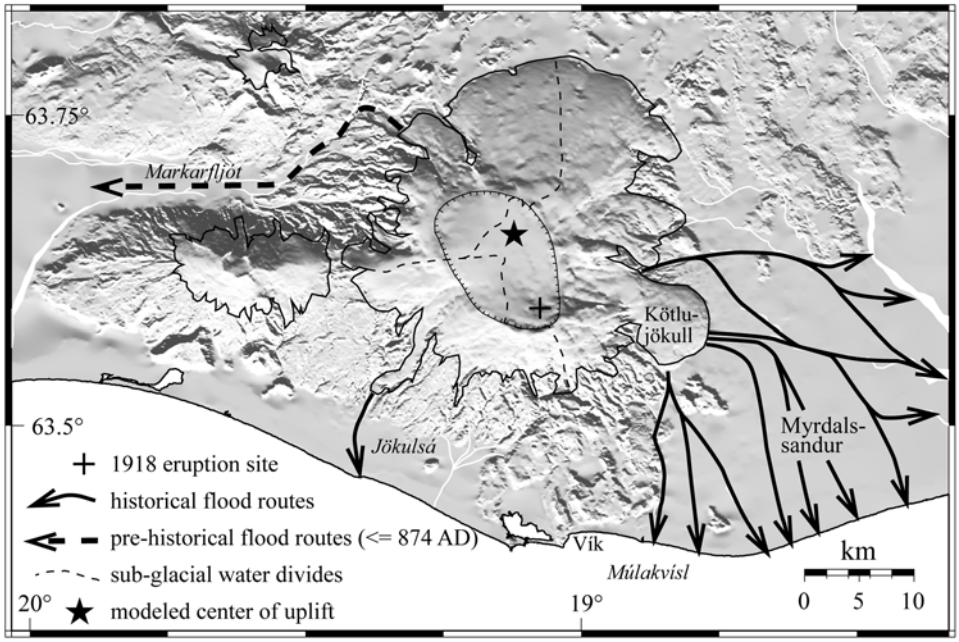

Figure 12. Sketch of jökulhlaup routes from the Mýrdalsjökull ice cap [*Larsen*, 2000]. The dashed lines on the ice surface depict subglacial water divides, as determined by *Björnsson et al.* [2000]. The modeled center of uplift is near to several subglacial water catchments. Floodwater might drain to either side of the ice cap, depending on the exact location of the eruption site within the caldera.

cantly on a timescale of thousands of years [*Óladóttir et al.*, 2008]. The existence of a magma chamber beneath the northern part of the caldera at the present time is therefore by no means excluded by the chemical data. The critical inflation level for this presently inflating magma chamber is unknown. It may be significantly lower than what the volume of the last previous eruption would imply.

[38] We note that the above estimate of the inflation volume is likely to be too high due to the effects of decreasing ice load. Similarly, the depth of the inflation source is likely to be over-estimated. Decreasing ice load will affect primarily the vertical component of the uplift signal. Therefore by removing the ice-load effect the remaining displacement field will imply a shallower inflation source. A depth of 2–3 km is consistent with the deformation data. The inflating body may therefore coincide with the body of low P-velocity and high S-wave attenuation identified beneath the caldera by *Gudmundsson et al.* [1994].

[39] The present episode of unrest in Katla is the longest known since the major eruption of 1918. Whether it leads to a large eruption remains to be seen. The most hazardous aspect of historical eruptions of Katla has been the large jökulhlaups caused by the melting of glacier ice during the beginning phase of the eruptions. The path of these outburst floods depends critically on the location of the eruption site within the caldera. The eruptions during historic time have originated in the eastern part of the caldera and consequently the floods have issued to the flood plane of Mýrdalssandur, SE of the volcano. The present water divides under the ice within the caldera have been mapped by *Björnsson et al.* [2000] (Figure 12). If the site of the next eruption is near the apex of the inflation bulge the next flood will similarly be issued to the SE. The apex is, however, very close to the water divide and slight shift in the eruption site will change the potential flood path dramatically. In addition, it is well known from other inflating volcanoes that the eruption site may not be located at the apex of the premonitory inflation bulge. The eruptions of Grímsvötn in 1998 and 2004, were, e.g., preceded by inflation centered on the caldera [*Sturkell et al.*, 2003b, 2006] and yet the eruption sites were located at the caldera rim. The eruptions of Krafla in the 1980ies were preceded by inflation of the caldera region but the eruptions were located on the transecting rift, some of them quite far from the caldera [e.g., *Einarsson*, 1991b; *Buck et al.*, 2006]. The location of the inflation bulge of Katla may therefore be of limited predictive value for the path of the next jökulhlaup.

16. Conclusions

[40] A study of seismic, geodetic, and glaciological data obtained in the last few decades leads us to the following

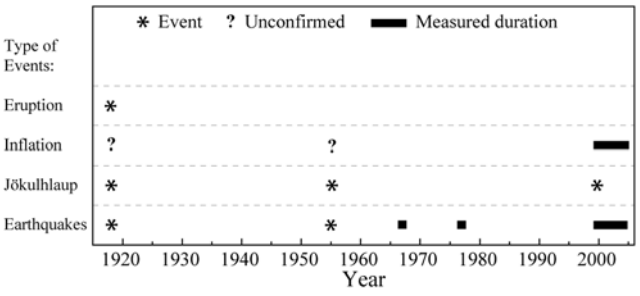

Figure 13. Schematic plot of the timing and the type of processes that have occurred during periods of volcanic unrest at Katla between 1918 and 2004. Note that only the duration of the 1999–2004 intrusion episode is known.

Table 3. Excess Melting Beneath Ice Cauldrons in the Period 2001–2004 (r: Cauldron Radius, Δh: Increase in Depth, $\Delta V = \pi r^2 \Delta h/3$ is Increase in Volume of Cauldron, Estimated as a Cone With Height Δh and Radius r)

Cauldron	r, m	Δh, m	ΔV, 10^6 m^3
10	400	6	1.0
11	300	7	0.7
14	700	5	2.5
15	400	10	1.7
16	500	13	3.4
Total			10.5

conclusions regarding the present state of the magma system of the Katla volcano:

[41] 1. The Katla volcano has been a persistent source of high seismic activity for at least half a century, or since a sensitive seismograph was installed in the region.

[42] 2. Four episodes of unusual activity can be identified after the 1918 eruption (Figure 13), probable small subglacial eruption in 1955, two episodes of greatly elevated seismicity in 1967 and 1976–77, and an episode of unrest that began in 1999 with a flash flood, probably as a result of a small subglacial eruption.

[43] 3. The present episode is characterized by elevated seismic activity, both in the caldera and in a dense epicentral cluster west of the caldera rim at Goðabunga. A slow inflation began with a center in the northern part of the caldera. GPS-points on nunataks near the caldera rim were displaced upwards and horizontally away from the center at a rate of 1–2 cm a^{-1}. This is taken as evidence of magma accumulation at a depth of less than 5 km beneath the caldera. Deepening of several depressions in the glacier surface indicates that the heat output of the volcano increased, probably as a consequence of the inflation.

[44] 4. The vertical movements by themselves could alternatively be explained by the reduction of the ice load of the glacier [*Pinel et al.*, 2007], but the horizontal movements cannot. We therefore prefer to interpret the inflation as the result of pressure increase in the roots of the volcano. A depth of 2–3 km is consistent with the deformation data, taking the ice load reduction into account.

[45] 5. The current episode of unrest of Katla was preceded by two intrusion events of the neighboring volcano Eyjafjallajökull, in 1994 and 1999. Eruptions of Eyjafjallajökull are known to have been previously associated with activity of Katla.

[46] 6. The intense seismic cluster at Goðabunga does not seem to produce a detectable deformation signal at our measuring stations that are all more than 8 km distant. This indicates that the source of the activity has to be shallow. A shallow, slowly migrating cryptodome, as has been postulated, can be reconciled with the data.

[47] 7. The total volume added to the Katla magma storage system since 1999 is of the order of 0.01 km^3. This is minute in comparison to the volume produced in the last major eruption. The volume of the 1918 products was of the order of 1 km^3.

[48] 8. The course of events during the present episode slowed down considerably in 2004. Nevertheless, the Katla volcano remains in an agitated state, the present episode is the longest recorded so far, and an eruption in the near future should not be ruled out.

[49] 9. If the location of the next volcanic eruption is at the inferred site of the center of volcanic uplift, then the resulting meltwater will drain beneath Kötlujökull to produce a jökulhlaup on Mýrdalssandur (Figure 12). However, the inferred center of uplift is near to three other subglacial water-divides [*Björnsson et al.*, 2000], thus making the routing of the consequent jökulhlaup highly sensitive to the location of the eruption site.

[50] **Acknowledgments.** We thank Benedikt Bragason and the rescue team in Vík for assistance with field logistics. Comments from the reviewers, Dave McGarvie and Thorvaldur Thordarson, have helped us to significantly improve the paper. Also the suggestions of the associate editor Sarah Fagents have been most helpful. This study was supported by the following institutions and research grants: the Icelandic Roads Authority; the Icelandic government; the University of Iceland Research Fund; the Icelandic research council (RANNÍS); and the European Union projects FORESIGHT (GOCE-CT-2003-511139) and VOLUME (018471). The figures were produced using the GMT public domain software [*Wessel and Smith*, 1998].

References

Bevington, P. R. (1969), *Data Reduction and Error Analysis*, McGraw-Hill, New York.

Björnsson, H. (2002), Subglacial lakes and jökulhlaups in Iceland, *Global Planet. Change*, *35*, 255–271.

Björnsson, H., F. Pálsson, and M. T. Guðmundsson (2000), Surface and bedrock topography of Mýrdalsjökull, South Iceland: The Katla caldera, eruption sites and routes of jökulhlaups, *Jökull*, *49*, 29–46.

Buck, W. Roger, P. Einarsson, and B. Brandsdóttir (2006), Tectonic stress and magma chamber size as controls on dike propagation: Constraints from the 1975–1984 Krafla rifting episode, *J. Geophys. Res.*, *111*, B12404, doi:10.1029/2005JB003879.

Dahm, T., and B. Brandsdóttir (1997), Moment tensors of microearthquakes from the Eyjafjallajökull volcano in South Iceland, *Geophys. J. Int.*, *130*, 183–192.

DeMets, C., R. G. Gordon, D. F. Argus, and S. Stein (1994), Effect of recent revision to the geomagnetic reversal time scale on estimates of current plate motions, *Geophys. Res. Lett.*, *21*, 2191–2194.

Dieterich, J. H., and R. W. Decker (1975), Finite element modelling of surface deformation associated with volcanism, *J. Geophys. Res.*, *80*, 4094–4102.

Eggertsson, S. (1919), Ýmislegt smávegis viðvíkjandi Kötlugosinu 1918, *Eimreiðin*, *25*, 212–222.

Einarsson, P. (1987), Compilation of earthquake fault plane solutions in the North Atlantic and Arctic Oceans, in *Recent Plate Movements and Deformation*, edited by K. Kasahara, pp. 47–62, Geodynamics Series, 20, Am. Geophys. Union.

Einarsson, P. (1991a), Earthquakes and present-day tectonism in Iceland, *Tectonophysics*, *189*, 261–279.

Einarsson, P. (1991b), The Krafla volcano-tectonic episode 1975–1989 (in Icelandic), in: Náttúra Mývatns, (ed. Á. Einarsson and A. Garðarsson), Hið Íslenska Náttúrufræðifélag, Reykjavík, pp. 97–139.

Einarsson, P. (2000), Atburðarás í tengslum við hlaup í Jökulsá á Sólheimasandi í júlí 1999 (Course of events associated with jökulhlaup in Jökulsá á Sólheimasandi in July 1999, abstract in Icelandic), Geoscience Society of Iceland, Special Conference, Feb. 17, 2000, Abstract Volume, p. 14.

Einarsson, P., and B. Brandsdóttir (2000), Earthquakes in the Mýrdalsjökull area, Iceland, 1978–1985: Seasonal correlation and relation to volcanoes, *Jökull*, *49*, 59–73.

Einarsson, P., and K. Sæmundsson (1987), Earthquake epicenters 1982–1985 and volcanic systems in Iceland (map), in *Í Hlutarsins Eðli: Festschrift for Thorbjorn Sigurgeirsson*, edited by Th. Sigfússon, Menningarsjóður, Reykjavík.

Einarsson, P., H. Soosalu, E. Sturkell, F. Sigmundsson, and H. Geirsson (2005), Virkni í Kötlueldstöðinni og nágrenni hennar síðan 1999 og hugsanleg þróun atburðarásar (Activity of Katla and surrounding area since 1999 and potential scenarios, in Icelandic), in *Hættumat vegna eldgosa og hlaupa frá vestanverðum Mýrdalsjökli og Eyjafjallajökli* (Assessment of hazard due to eruptions and jökulhlaups from western Mýrdalsjökull and Eyjafjallajökull), edited by M. T. Guðmundsson and Á. G. Gylfason, pp. 151–158, University Publ., Reykjavík, Iceland.

Einarsson, P., F. Sigmundsson, E. Sturkell, Þ. Árnadóttir, R. Pedersen, C. Pagli, H. Geirsson (2006), Geodynamic signals detected by geodetic methods in Iceland, In: C. Hirt (editor), Festschrift for Prof. G. Seeber,

Wissenschaftliche Arbeiten der Fachrichtung Geodäsie und Geoinformatik der Universität Hannover Nr. 258, 39–57.

Elíasson, J., G. Larsen, M. T. Gudmundsson, and F. Sigmundsson (2006), Probabilistic model for eruptions and associated flood events in the Katla caldera, Iceland, *Comput. Geosci.*, *10*, 179–200.

Geirsson, H., Th. Arnadóttir, C. Völksen, W. Jiang, E. Sturkell, T. Villemin, P. Einarsson, F. Sigmundsson, and R. Stefánsson (2006), Current plate movements across the Mid-Atlantic Ridge determined from 5 years of continuous GPS measurements in Iceland, *J. Geophys. Res.*, *111*, B09407, doi:10.1029/2005JB003717.

Grapenthin, R., F. Sigmundsson, H. Geirsson, T. Arnadottir, and V. Pinel (2006), Icelandic rhythmics: Annual modulation of land elevation and plate spreading by snow load, *Geophys. Res. Lett.*, *33*, L24305, doi:10.1029/2006GL028081.

Gudmundsson, Ó., B. Brandsdóttir, W. Menke, and G. E. Sigvaldason (1994), The crustal magma chamber of the Katla volcano in south Iceland revealed by 2-D seismic undershooting, *Geophys. J. Int.*, *119*, 277–296.

Gudmundsson, M. T., F. Sigmundsson, H. Björnsson, and Þ. Högnadóttir (2004), The 1996 eruption at Gjálp, Vatnajökull ice cap, Iceland: Course of events, efficiency of heat transfer, ice deformation and subglacial water pressure, *Bull. Volcanol.*, *66*, doi:10.1007/s00445-003-0295-9.

Gudmundsson, M. T., Þ. Högnadóttir, A. B. Kristinsson, and S. Gudbjörnsson (2007), Geothermal activity in the subglacial Katla caldera, Iceland, 1999–2005, studied with radar altimetry, *Ann. Glaciol.*, *45*, 66–72.

Haraldsson, H. (1981), The Markarfljót sandur area, southern Iceland, sedimentological, petrological and stratigraphic studies, *Striae*, *15*, 1–58.

Hugentobler, U., S. Schaer, and P. Fridez (2001), Bernese GPS software version 4.2, Astron. Inst., Univ. of Bern, Bern, Switzerland.

Jarosch, A. H., and M. T. Gudmundsson (2007), Numerical studies of ice flow over subglacial geothermal heat sources at Grímsvötn, Iceland, using the full Stokes equations, *J. Geophys. Res.*, *112*(F2), F02008, doi:10.1029/2006JF000540.

Jóhannesson, H., S. P. Jakobsson, and K. Saemundsson (1990), Geological map of Iceland, sheet 6, South-Iceland, third edition, Icelandic Museum of Natural History and Geodetic Survey, Reykjavík.

Jóhannsson, G. (1919), *Kötlugosið 1918*. (The Katla eruption of 1918, in Icelandic). Bókaverslun Ársæls Árnasonar, Reykjavík, p. 72.

Jónsdóttir, K., A. Tryggvason, R. Roberts, B. Lund, H. Soosalu, and R. Böðvarsson (2007), Habits of a glacier-covered volcano: Seismicity patterns and velocity structure of Katla volcano, Iceland, *Ann. Glaciol.*, *45*, 169–177.

Jónsson, G., and L. Kristjánsson (2000), Aeromagnetic measurements over Mýrdalsjökull and vicinity, *Jökull*, *49*, 47–58.

Lacasse, C., H. Sigurdsson, S. N. Carey, H. Jóhannesson, L. E. Thomas, and N. W. Rogers (2007), Bimodal volcanism at the Katla subglacial caldera, Iceland: Insight into the geochemistry and petrogenesis of rhyolitic magmas, *Bull. Volcanol.*, *69*, 373–399, doi:10.1007/s00445-006-0082-5.

LaFemina, P. C., T. H. Dixon, R. Malservisi, T. Árnadóttir, E. Sturkell, F. Sigmundsson, and P. Einarsson (2005), Geodetic GPS Measurements in South Iceland: Strain accumulation and partitioning in a propagating ridge system, *J. Geophys. Res.*, *110*, B11405, doi:10.1029/2005JB003675.

Larsen, G. (2000), Holocene eruptions within the Katla volcanic system, south Iceland: Characteristics and environmental impact, *Jökull*, *49*, 1–28.

Larsen, G., A. J. Dugmore, and A. J. Newton (1999), Geochemistry of historical-age silicic tephras in Iceland, *Holocene*, *9*, 463–471.

Larsen, G., K. T. Smith, A. Newton, and Ó. Knudsen (2005), Jökulhlaup til vesturs frá Mýrdalsjökli: Ummerki um forsöguleg hlaup niður Markarfljót (Jokulhlaups towards west from Mýrdalsjökull, evidence for prehistoric floods in Markarfljót river, in Icelandic), in *Hættumat vegna eldgosa og hlaupa frá vestanverðum Mýrdalsjökli og Eyjafjallajökli* (Assessment of hazard due to eruptions and jökulhlaups from western Mýrdalsjökull and Eyjafjallajökull), edited by M. T. Guðmundsson and Á. G. Gylfason, pp. 75–98, University Publ., Reykjavík, Iceland.

Major, J. J., and C. G. Newhall (1989), Snow and ice perturbation during historical volcanic eruptions and the formation of lahars and floods, *Bull. Volcanol.*, *52*, 1–27.

Óladóttir, B. A., G. Larsen, Th. Thordarson, and O. Sigmarsson (2005), The Katla volcano, S-Iceland: Holocene tephra stratigraphy and eruption frequency, *Jökull*, *55*, 53–74.

Óladóttir, B. A., O. Sigmarsson, G. Larsen, and Th. Thordarson (2008), Katla volcano, Iceland: Magma composition, dynamics and eruption frequency as depicted by the Holocene tephra layer record, *Bull. Volc.*, *70*, 473–493.

Óskarsson, N., G. E. Sigvaldason, and S. Steinthórsson (1982), A dynamic model of rift zone petrogenesis and the regional petrology of Iceland, *J. Petrol.*, *23*, 28–74.

Pedersen, R., and F. Sigmundsson (2004), InSAR based sill model links spatially offset areas of deformation and seismicity for the 1994 unrest episode at Eyjafjallajökull volcano, Iceland, *Geophys. Res. Lett.*, *31*, L14610, doi:10.1029/2004GL020368.

Pedersen, R., and F. Sigmundsson (2006), Temporal development of the 1999 intrusive episode in the Eyjafjallajökull volcano, Iceland, derived from InSAR images, *Bull. Volcanol.*, *68*, 377–393, doi:10.1007/s00445-005-0020-y.

Pinel, V., F. Sigmundsson, E. Sturkell, H. Geirsson, P. Einarsson, M. T. Gudmundsson, and T. Högnadóttir (2007), Green's function estimates of Earth response to variable surface loads: Application to deformation of the subglacial Katla volcano, Iceland, *Geophys. J. Int.*, *169*, 325–338, doi:10.1111/j.1365-246X.2006.03267.x.

Rist, S. (1967), Jökulhlaups from the ice cover of Mýrdalsjökull on June 25, 1955 and January 20, 1956, *Jökull*, *17*, 243–248.

Roberts, M. J. (2005), Jökulhlaups: A reassessment of floodwater flow through glaciers, *Rev. Geophys.*, *43*, RG1002, doi:10.1029/2003RG000147.

Roberts, M. J., F. S. Tweed, A. J. Russell, O. Knudsen, and T. D. Harris (2003), Hydrological and geomorphic effects of temporary ice-dammed lake formation during jökulhlaups, *Earth Surf. Processes Landforms*, *28*, 723–737.

Rögnvaldsson, S. T., and R. Slunga (1993), Routine fault plane solutions for local networks: A test with synthetic data, *Bull. Seismol. Soc. Am.*, *83*, 1232–1247.

Sigmundsson, F. (2006), *Iceland Geodynamics, Crustal Deformation and Divergent Plate Tectonics.* Springer–Praxis Publishing Ltd, Chichester, 209 pp.

Sigmundsson, F., P. Einarsson, R. Bilham, and E. Sturkell (1995), Rift-transform kinematics in south Iceland: Deformation from Global Positioning System measurements, 1986 to 1992, *J. Geophys. Res.*, *100*, 6235–6248.

Sigurðsson, O. (2003), Jöklabreytingar 1930–1960, 1960–1990 og 2000–2001, *Jökull*, *52*, 61–67.

Sigurðsson, O., S. Zóphoníasson, and E. Ísleifsson (2000), Jökulhlaup úr Sólheimajökli 18. júlí 1999 (The jökulhlaup from Sólheimajökull July 18, 1999, in Icelandic with English summary), *Jökull*, *49*, 75–80.

Sinton, J. M., D. S. Wilson, D. M. Christie, R. N. Hey, and J. R. Delaney (1983), Petrological consequences of rift propagation on oceanic spreading ridges, *Earth Planet. Sci. Lett.*, *62*, 193–207.

Smith, K. (2004), Holocene jökulhlaups, glacier fluctuations and palaeoenvironment, Mýrdalsjökull, South Iceland, PhD thesis 139 pp. Edinburgh Univ.

Smith, K. T., and A. J. Dugmore (2006), Mid- to late first millennium AD floods in South Iceland and their implications for landscapes of settlement, *Geografiska Annaler*, *88 A*(2), 165–176.

Soosalu, H., K. Jónsdóttir, and P. Einarsson (2006), Seismicity crisis at the Katla volcano, Iceland—signs of a cryptodome?, *J. Volcanol. Geotherm. Res.*, *153*, doi:10.1016/j.jvolgeores.2005.10.013.

Sturkell, E., F. Sigmundsson, and P. Einarsson (2003a), Recent unrest and magma movements at Eyjafjallajökull and Katla volcanoes, Iceland, *J. Geophys. Res.*, *108*(B8), 2369, doi:10.1029/2001JB000917.

Sturkell, E., P. Einarsson, F. Sigmundsson, S. Hreinsdóttir, and H. Geirsson (2003b), Deformation of Grímsvötn volcano, Iceland: 1998 eruption and subsequent inflation, *Geophys. Res. Lett.*, *30*(4), 1182, doi:10.1029/2002GL016460.

Sturkell, E., P. Einarsson, F. Sigmundsson, H. Geirsson, R. Pedersen, E. Van Dalfsen, A. Linde, S. Sacks, and R. Stefánsson (2006), Volcano geodesy and magma dynamics in Iceland, *J. Volcanol. Geotherm. Res.*, *150*, doi:10.1016/j.jvolgeores.2005.07.010.

Sveinsson, G. (1919), *Kötlugosið 1918 og afleiðingar þess* (The Katla eruption of 1918 and its consequences, in Icelandic). Prentsmiðja Gutenbergs, Reykjavík, pp. 61.

Thorarinsson, S. (1975), Katla og annáll Kötlugosa (Katla and annals of its eruptions, in Icelandic), In *Árbók Ferðafélags Íslands*, Reykjavík, 125–149.

Thordarson, T., D. J. Miller, G. Larsen, S. Self, and H. Sigurdsson (2001), New estimates of sulfur degassing and atmospheric mass-loading by the 934 AD Eldgjá; eruption, Iceland, *J. Volcanol. Geotherm. Res.*, *108*, 33–54.

Thoroddsen, Þ. (1925), Die Geschichte der Isländischen Vulkane (The history of Icelandic volcanoes, in German). The Royal Danish Science Society Skrifter, Department of Nat. Sciences and Mathematics, 8. Række, IX, 458 pp.

Tómasson, H. (1996), The jökulhlaup from Katla in 1918, *Ann. Glaciol.*, *22*, 249–254.

Tryggvason, E. (1960), Earthquakes, jökulhlaups and subglacial eruptions, *Jökull*, *10*, 18–22.

Tryggvason, E. (1973), Surface deformation and crustal structure in the Mýrdalsjökull area of south Iceland, *J. Geophys. Res.*, *78*, 2488–2497.

Tryggvason, E. (2000), Ground deformation at Katla: Results of precision levelling 1967–1995, *Jökull*, *48*, 1–8.

Vogfjörð, K. S. (2002), Var eldgos orsök jarðskjálftaóróans í Sólheimajökulshlaupinu, 17 júlí 1999? (Was volcanic tremor during the jökulhlaup from Sólheimajökull on 17 July 1999 caused by an eruption? In Icelandic), Geoscience Society of Iceland, Abstract Volume, p. 32.

Wessel, P., and W. H. F. Smith (1998), New, improved version of generic mapping tools released, *Eos Trans. AGU*, *79*(47), 579.

P. Einarsson and M. T. Gudmundsson, Institute of Earth Sciences, University of Iceland, Sturlugata 7, 101 Reykjavík, Iceland. (palli@raunvis.hi.is; mtg@raunvis.hi.is)

H. Geirsson, G. B. Guðmundsson, and M. J. Roberts, Physics Department, Icelandic Meteorological Office, Bústaðavegur 9, 150 Reykjavík, Iceland. (dori@vedur.is; gg@vedur.is; matthew@vedur.is)

H. Ólafsson, F. Sigmundsson, and E. Sturkell, Nordic Volcanological Center, Institute of Earth Sciences, University of Iceland, Sturlugata 7, 101 Reykjavík, Iceland. (hallo@hi.is; fs@hi.is; sturkell@hi.is)

V. Pinel, LGIT-Universite de Savoie Campus Scientifique, 73376 Le Bourget du Lac Cedex, France. (virginie.pinel@univ-savoie.fr)

R. Stefánsson, Department of Business and Natural Sciences, University of Akureyri, 600 Akureyri, Iceland. (raha@simnet.is)